Available online at www.sciencedirect.com
ScienceDirect
Trans. Nonferrous Met. Soc. China 33(2023) 315−324
Transactions of Nonferrous Metals Society of China
www.tnmsc.cn

Reductive leaching kinetics of indium and further selective separation by fraction precipitation

Cun-xiong LI, Zhao-yan ZHANG, Yao-yang ZHANG, Zhi-gan DENG, Wen-bin JI, Xiao-tan LIN

Faculty of Metallurgical and Energy Engineering,
Kunming University of Science and Technology, Kunming 650093, China

Received 30 September 2021; accepted 7 April 2022

Abstract: Reductive leaching of high-iron bearing zinc leaching residue (HIZLR) by zinc sulfide concentrate to extract indium and its further selective separation from the leachate were studied. The results indicated that over 95% of indium extraction was achieved at particle sizes of 74−105 μm, reaction temperature of 90 °C, leaching time of 300 min and sulfuric acid concentration of 1.4 mol/L. The leaching kinetics was analyzed by the shrinking core model, and the leaching data from various experimental conditions indicated that the reactions were controlled by the diffusion through the solid product layer with an activation energy of 17.96 kJ/mol. The order of the reaction with respect to the sulfuric acid concentration was determined to be 2.41. Over 99% of copper and arsenic were coprecipitated in the cementation of copper with iron powder. More than 98% of indium was selectively separated from zinc sulfate solution with high ferrous ion content, and the indium-rich precipitate, which had an indium content of approximately 2.4%, could be further treated by the acid leaching−solvent extraction−electrowinning process to produce pure indium.
Key words: reductive leaching; high iron zinc leaching residue; zinc sulfide concentrate; kinetics; indium precipitation

1 Introduction

Indium is an important metal used in high-tech fields, such as computer science, defense, military, and modern information industries [1,2]. However, there are very few mineral types rich in indium, and they rarely occur in nature. Indium is most commonly found in association with zinc-bearing minerals, such as sphalerite and marmatite [3,4]. At present, more than 80% of the world's zinc is produced by the roasting−leaching−purification−electrowinning process, and over 98% of indium present in zinc sulfide concentrate is transferred into the leaching residue [5−7]. This residue, which contains heavy metals or toxic elements, such as zinc, indium, copper, lead and arsenic, is environmentally unacceptable and is classified as a hazardous waste [8−10]. Leaching zinc and indium from zinc leaching residue (ZLR) is challenging because it is mostly associated with stable spinel zinc ferrites [11]. High pressure leaching [12,13], oxidative leaching [14,15], mechanical activation leaching [16] and bio- leaching [17,18] have been proposed to effectively extract zinc and indium from indium containing ZLR or zinc sulfide concentrate.

Kinetic analysis of solid−fluid heterogeneous reactions is of great importance at the industrial level, as this is the basis for scale-up and reactor designs [11,19]. A few researchers [20−23] have reported the indium leaching kinetics from different indium containing materials. However, based on the component and phase composition in indium containing materials, the leaching kinetics and extraction efficiency of indium varies. It was reported that indium leached from synthetic indium-bearing zinc ferrite was controlled by the

Corresponding author: Cun-xiong LI, Tel: +86-13518764748, E-mail: licunxiong@126.com
DOI: 10.1016/S1003-6326(22)66109-0

chemical reactions with activation energy of 68.8 kJ/mol [22]. Indium leached from zinc plant leaching residue was controlled by chemical reactions in the early stage, evolved to a mix-controlled stage, and finally to the stage in which diffusion was controlled by the solid product layer. The activation energy was 46.09 kJ/mol in the chemical reaction control stage and 11.62 kJ/mol in the later product layer diffusion-controlled stage [24]. Therefore, it can be concluded that the indium leaching efficiency and kinetic models are strongly dependent on the phase composition of the particular materials.

In Southwest China, a lot of ZLR with high indium (>800 g/t) and iron (>30%) contents are produced by local zinc refineries. Recovery of indium is necessary and important both from an economic point of view and the increased requirements for environmental protection. In the conventional hot acid leaching process, most of the valuable metals are extracted from ZLR. Iron, which is mostly in its ferric form in the leachate, presents a serious challenge for the selective recovery of indium by cementation or solvent extraction from the leaching solution, and ferric ions should be reduced to ferrous ions. These challenges result in high reducing agent consumption and operation cost when ZLR with high iron content is treated. In this work, the reductive leaching−fraction precipitation process is proposed to recover indium from high-iron bearing zinc leach residue (HIZLR). Firstly, HIZLR is leached using zinc sulfide concentrate as reducing agent to obtain the maximum extraction of indium from the residue, and ferric ions are simultaneously reduced to ferrous ions under acidic conditions by the sulfide present in the concentrate. Secondly, the reductive leachate, which also has a high copper content, is treated to recover copper and indium by fraction precipitation. The fraction precipitation process includes the following steps: (1) copper precipitation by iron powder, (2) adjustment of the solution pH, and (3) indium precipitation from the pH-adjusted leachate by zinc powder.

The main objectives of this study are investigation of the effects of stirring speed, particle size, reaction temperature and sulfuric acid concentration on the indium leaching efficiency from HIZLR, development of the optimum conditions for the extraction of indium and the reaction kinetics using different kinetic models, and study of the selective separation of copper and indium from reductive leachate by fraction precipitation.

2 Experimental

2.1 Material feed and mineralogical analysis

The HIZLR, zinc sulfide concentrate and zinc calcine used in the present study were collected from a zinc refinery in Southwest of China. The elemental composition of these materials is given in Table 1. The zinc, indium, and iron contents in the materials with different size fractions are presented in Table 2. Mineralogical analysis of the samples was performed by XRD, and the results are shown in Figs. 1, 2 and 3.

As given in Table 1, the HIZLR contains 25.45 wt.% zinc, 34.73 wt.% iron and 853.6 g/t indium. Minor amounts of other heavy metals, such

Table 1 Elemental composition of experimental materials (wt.%)

Component	Zn	Fe	In	S	Cu	Pb	Sn	Ag	SiO_2
HIZLR	25.45	34.73	853.6*	3.52	1.47	0.172	0.113	73.14*	5.44
Zinc sulfide concentrate	45.37	16.82	386.7*	32.31	0.96	0.081	0.069	43.68*	2.43
Zinc calcine	49.2	14.56	418.3*	3.19	1.02	0.67	0.043	108.7*	2.77

*−g/t

Table 2 Chemical composition of samples with different size fractions

Size fraction/μm	HIZLR			Zinc sulfide concentrate		
	w(Zn)/%	*w*(In)/(g·t^{-1})	*w*(Fe)/%	*w*(Zn)/%	*w*(In)/(g·t^{-1})	*w*(Fe)/%
105−150	25.07	838.3	34.35	45.22	325.5	15.43
74−105	25.22	828.4	34.67	45.36	382.6	15.38
53−74	25.49	863.7	34.74	45.24	400.7	17.46
43−53	25.46	857.6	34.03	45.72	379.3	16.84

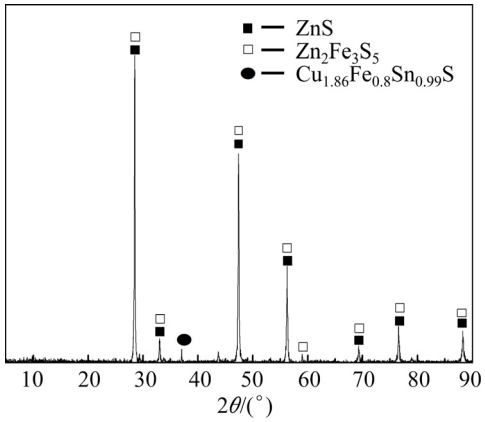

Fig. 1 XRD pattern of zinc sulfide concentrate

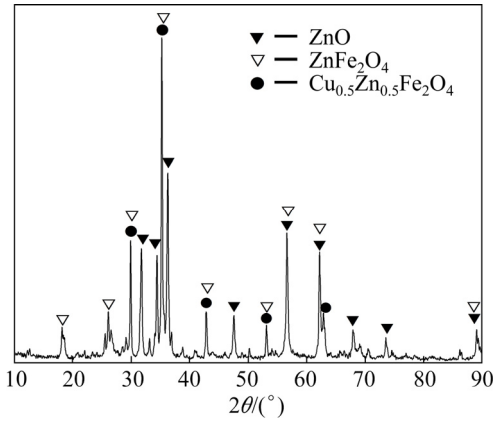

Fig. 2 XRD pattern of zinc calcine

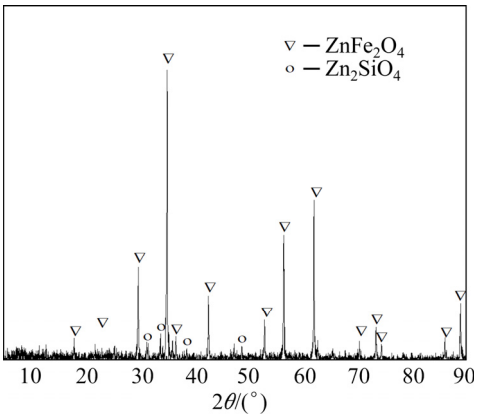

Fig. 3 XRD pattern of HIZLR

as copper, lead, and tin are also detected. The iron content in zinc sulfide concentrate is 16.82 wt.%, which is much higher than that in conventional zinc ore (3−8 wt.%) [25,26]. HIZLR is produced from the roasted zinc sulfide concentrate under conditions in industrial practice.

Figure 1 shows that the main mineralogical phases in zinc sulfide concentrate are sphalerite and marmatite, with a small quantity of polymetallic sulfide. As shown in Fig. 2, zinc ferrite or copper ferrite is formed during the roasting process of zinc sulfide concentrate. Undissolved zinc ferrite and a small amount of zinc silicate are detected in HIZLR (Fig. 3). No special indium-bearing minerals are identified due to trace amounts of indium in both zinc sulfide concentrate and HIZLR.

In all leaching experiments, spent electrolyte containing 185.6 g/L H_2SO_4 and 52.33 g/L Zn^{2+} was used as the leaching agent. Sodium lignosulfonate lignin was added at 100 g/t as a sulfur dispersant. Analytical grade iron powder (Fe 99.5%) and zinc powder (Zn 99.0%) were used as sacrificial metals for copper and indium removal, respectively.

2.2 Reductive leaching−fraction precipitation process

2.2.1 Reductive leaching

Leaching experiments were performed in a three-necked 2 L capacity glass reactor with a mechanical stirrer, a sample collection tube, and a condenser tube to prevent evaporation loss. Spent electrolyte required was transferred to the reactor and placed in the water bath. After the test temperature was reached, 100 g HIZLR and 25 g zinc sulfide concentrate were added to the reactor. Then, the solution was agitated at the desired agitation speed. During each experiment, the samples were collected at regular intervals and filtered on a Buchner vacuum filter to separate the liquor from the slurry. The solids were washed and subsequently dried at 80 °C before analysis. The liquids were analyzed to determine the indium concentrations. The liquid to solid ratio was maintained constantly at 11:1 g/mL for all experiments.

The indium leaching efficiency (x_i) was calculated by Eq. (1):

$$x_i = V_0 C_i / (m_1 c_1 + m_2 c_2) \quad (1)$$

where V_0 is the initial volume (mL) of the solution, C_i is the concentration of indium in the Sample i (mg/L), m_1 is the mass (mg) of HIZLR, m_2 is the mass (mg) of zinc sulfide concentrate, c_1 is the content of indium in HIZLR (wt.%), and c_2 is the content of indium in zinc sulfide concentrate (wt.%). It must be noted that zinc and copper are also dissolved.

2.2.2 Fraction precipitation

The reductive leachate was treated in three steps: the precipitation of copper by iron powder,

pre-neutralization of free acid with zinc calcine and indium precipitation with zinc powder.

The copper and indium recovery from the reductive leachate were preceded by fractional precipitation with the addition of different chemical agents. Initially, copper was recovered by adding iron powder. Then, the pH of the copper precipitation supernatant was adjusted to 4.0 with the addition of zinc calcine to neutralize the free acid and minimize the zinc powder consumption in the next zinc precipitation step. Finally, indium was recovered from the pH-adjusted leachate by the addition of zinc powder.

The copper or indium precipitation rate (x) was calculated by Eq. (2):

$$x = (C_1V_1 - C_2V_2)/C_1V_1 \quad (2)$$

where C_1 is the initial concentration of copper or indium (g/L) in the sample solution, V_1 is the initial volume (L) of the sample solution, C_2 is the unprecipitated copper or indium concentration (g/L) in the supernatant after precipitation and V_2 is the volume (L) of the supernatant produced in the precipitation process.

2.3 Characterization and analysis

The elemental compositions of HIZLR, zinc sulfide concentrate and zinc calcine were detected by selective leaching. The elemental concentrations in solution were determined by ICP with mass spectrometric detection. Solid materials were characterized by X-ray diffraction (XRD) to identify their phases. The morphology and surface composition of the reductive leaching product were detected by scanning electron microscopy with energy dispersive spectrometry (SEM−EDS).

3 Results and discussion

3.1 Reductive leaching and kinetics analysis of indium leaching

3.1.1 Effect of stirring speed

The influence of stirring speed on the leaching efficiency of indium was studied by increasing the stirring speed from 100 to 400 r/min, and the results are shown in Fig. 4.

It is shown in Fig. 4 that the increase in stirring speed from 100 to 300 r/min produced an obvious increase in the leaching efficiency of indium. Thereafter, there is little effect on indium extraction when the stirring speed is increased from 300 to 400 r/min. The results show that the distribution of H^+ and the suspension of particles at 300 r/min or above are adequate. Thus, a stirring speed of 300 r/min was chosen for subsequent experiments. However, limit of the stirring speed does not imply that diffusion could not be a rate controlling step; it only means that at a high stirring speed, the hydrodynamic boundary layer around the particles reaches a limiting value. Thus, diffusion across this minimum thickness boundary layer could still be the slow step. Therefore, additional experimental evidence of activation energy is needed to ascertain the rate limiting step.

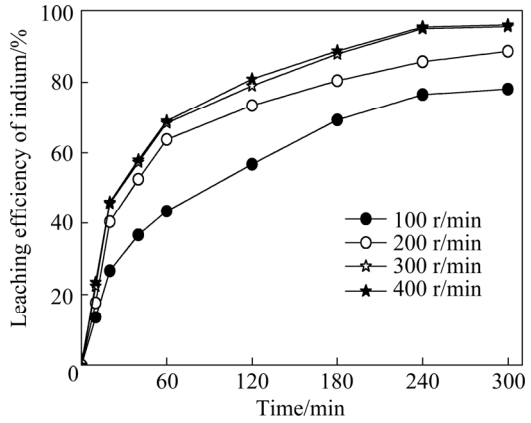

Fig. 4 Effect of stirring speed on indium extraction (particle size 74−105 μm, temperature 90 °C, and sulfuric acid concentration 1.4 mol/L)

3.1.2 Effect of particle size

The effect of particle size on the leaching efficiency of indium was studied using different size fractions (43−53, 53−74, 74−105 and 105−150 μm), and the results are shown in Fig. 5.

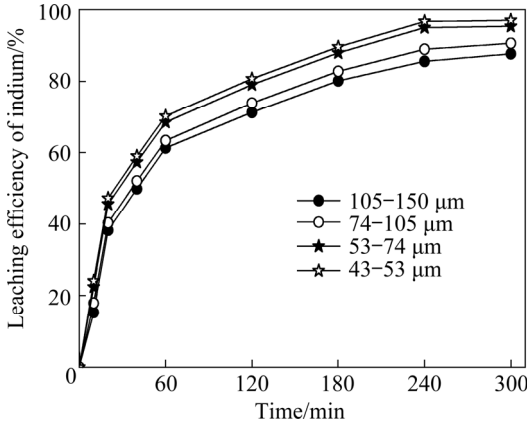

Fig. 5 Effect of particle size on indium extraction (stirring speed 300 r/min, temperature 90 °C, and sulfuric acid concentration 1.4 mol/L)

As is shown in Fig. 5, the decrease in particle size enhanced indium dissolution, although indium extraction with a particle size between 43 and 53 μm is only 9% higher than that with 105−150 μm particles. Many literature examples show that the smaller the particle size, the faster the reaction rate [27,28]. Therefore, the particle size of 74−105 μm was chosen.

3.1.3 Effect of temperature

The effect of the reaction temperature was studied over the range of 60−90 °C. The results presented in Fig. 6 show that the leaching efficiency of indium is strongly dependent on the temperature. When the temperature increased from 60 to 90 °C, the leaching rate of indium greatly increased from 70.7% to 95.7%.

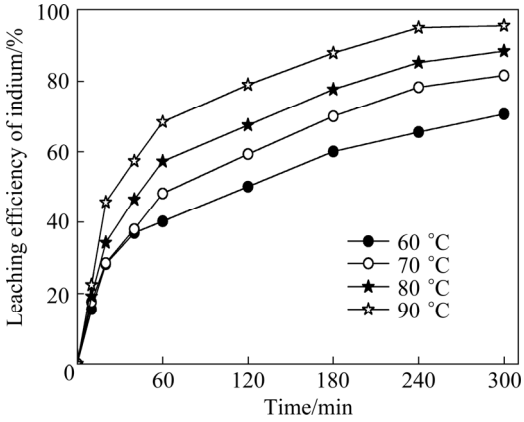

Fig. 6 Effect of temperature on indium extraction (stirring speed 300 r/min, particle size 74−105 μm, and sulfuric acid concentration 1.4 mol/L)

3.1.4 Effect of sulfuric acid concentration

To investigate the influence of the sulfuric acid concentration on indium extraction, experiments were carried out in solutions containing different initial sulfuric acid concentrations of 0.9, 1.1, 1.3, 1.4, and 1.8 mol/L. As seen in Fig. 7, increasing the sulfuric acid concentration significantly affected the indium leaching rate. Indium extraction increased from 48.9% to 95.6% when the concentration of sulfuric acid increased from 0.9 to 1.8 mol/L. It can also be observed that over 90% of indium was extracted at sulfuric acid concentration of 1.4 mol/L or above in approximately 240 min.

3.1.5 Characterization of leaching products

In the reductive leaching process, zinc ferrite present in HIZLR is dissolved by sulfuric acid and the ferric ions are reduced to ferrous ions by the sulfide present in zinc sulfide concentrate:

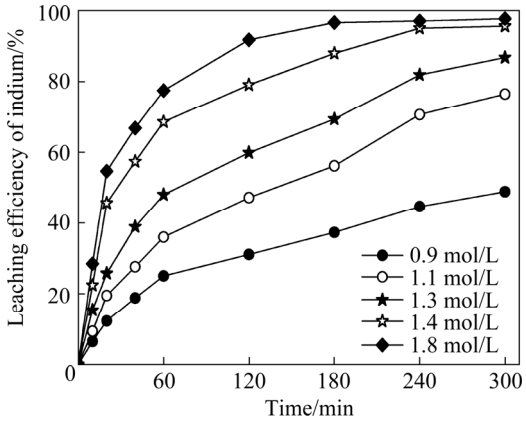

Fig. 7 Effect of sulfuric acid concentration on indium extraction (stirring speed 300 r/min, particle size 74−105 μm, and temperature 90 °C)

$$ZnFe_2O_4+4H_2SO_4+ZnS= 2ZnSO_4+2FeSO_4+S^0+4H_2O \quad (3)$$

Low concentrations of indium in HIZLR could be part of the zinc ferrite lattice or a coprecipitate as a hydroxide.

According to the reductive leaching reaction (3), the leaching residues contain elemental sulfur, and reductive leaching residues obtained at various reaction time were analyzed by XRD to determine the formation of elemental sulfur as a reaction product.

Figure 8 shows the XRD patterns of two residues obtained at 60 and 180 min. The residues were obtained at a stirring speed of 300 r/min, particle size of 74−105 μm, temperature of 90 °C and sulfuric acid concentration of 1.4 mol/L. The patterns in Fig. 8 clearly show diffraction peaks for elemental sulfur. The patterns for elemental sulfur at 180 min show stronger peaks compared to the

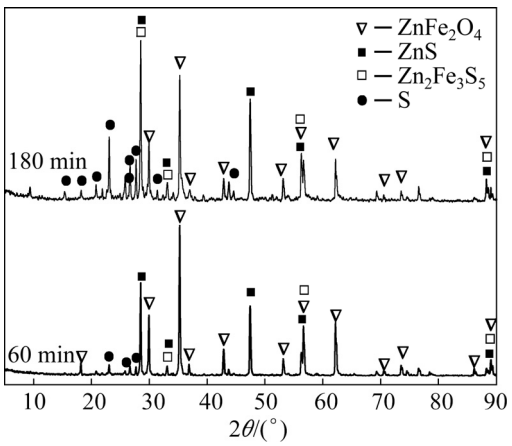

Fig. 8 XRD patterns of leaching residues obtained at different time

patterns at 60 min, which indicates that more elemental sulfur was formed with the progress of the reductive leaching reaction. In addition, diffraction peaks for undissolved zinc ferrite ($ZnFe_2O_4$), sphalerite (ZnS) and marmatite ($Zn_2Fe_3S_5$) were present in all the XRD patterns of the leaching residues.

The reductive leaching residue was detected with SEM−EDS to determine the morphology and occurrence states of the main components, and the results are shown in Fig. 9 and Table 3.

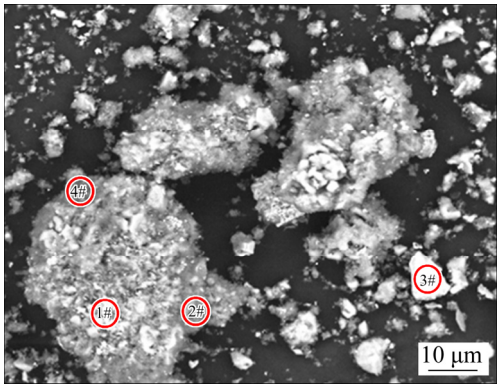

Fig. 9 SEM image of reductive leaching residue (stirring speed 300 r/min, particle size 74−105 μm, temperature 90 °C, sulfuric acid concentration 1.4 mol/L, and reaction time 180 min)

Table 3 Chemical composition of selected particles shown in Fig. 9 (wt.%)

Spot	Zn	Fe	Si	S	O
1	4.51	2.96	10.97	56.26	22.93
2	43.22	12.75	1.70	29.39	11.32
3	7.90	5.75	19.10	13.52	34.14
4	34.01	37.0	1.12	0.007	25.15

It can be found in Fig. 9 that the solid particles have rough and porous surfaces generated by the leaching process. According to Table 3, the main phase in Spot 1 is elemental sulfur owing to high sulfur content. Spot 2, which has a large proportion of S and Zn, can be identified as undissolved sphalerite. Spot 3 is mainly composed of O, Si and S, confirming the presence of quartz and elemental sulfur. Similarly, the main phase of Spot 4 is zinc ferrite. It is worth noting that the particle surfaces of undissolved zinc ferrite and sphalerite are covered by elemental sulfur. Therefore, it is proposed that the indium dissolution process could be controlled by diffusion of the reagent in the elemental sulfur layer on the particle surface.

3.1.6 Kinetics of indium dissolution in reductive leaching process

Indium dissolution from HIZLR and zinc sulfide concentrate can proceed in a heterogeneous manner, with a progressively thickening layer of insoluble product, while the thickness of the inner core of unreacted particles decreases.

Considering the morphology of the reductive leaching residue particles shown in Fig. 9, the experimental data can be analyzed by the shrinking core model in Fig. 10. The shrinking core model reveals that the rate-controlling step of the reaction process is the chemical reaction on the particle surface, the diffusion through the product layer, or a combination of both.

If indium dissolution is controlled by the chemical reaction at the mineral's surface, then the kinetics is determined by Eq. (4):

$$1-(1-x)^{1/3}=k_c\cdot t \tag{4}$$

where x is the fraction of indium reacted, t is the leaching time (min) and k_c is the chemical reaction rate constant.

Likewise, if the reaction rate is controlled by the diffusion of the leaching agent through the solid product layer around the unreacted core, then Eq. (5) is applied to determining the kinetics:

$$1-2/3x-(1-x)^{2/3}=k_d\cdot t \tag{5}$$

where k_d is solid product layer diffusion rate constant.

The relationships among $1-(1-x)^{1/3}$, $1-2/3x-(1-x)^{2/3}$ and the experimental data (Fig. 6) over time are plotted in Figs. 11 and 12, respectively.

The results presented in Figs. 11 and 12 show that the solid product diffusion model had a higher regression coefficient (R^2) at different temperatures.

The experimental results for the various conditions plotted according to the solid product diffusion model are shown in Figs. 13−15. It can be seen that the model fits the data well. From the slope of the curves in Fig. 12, the apparent kinetic constants at various temperatures can be determined, which were used to draw an Arrhenius plot, as shown in Fig. 16. The calculated activation energy (E_a) was 17.96 kJ/mol, which is a typical value for a process controlled by diffusion of a leaching agent through a solid product layer.

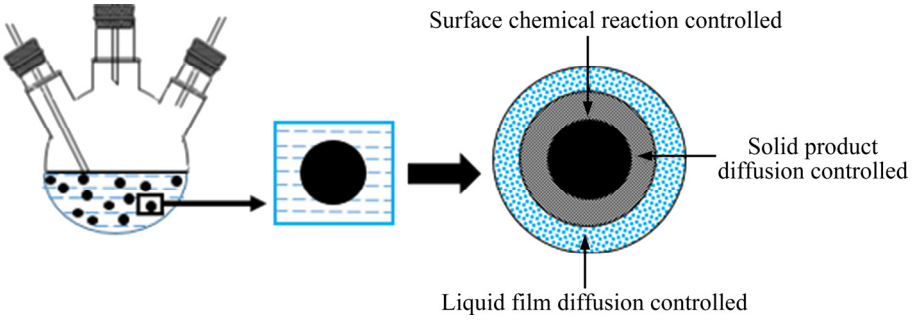

Fig. 10 Schematic diagram depicting various shrinking core kinetic phenomena

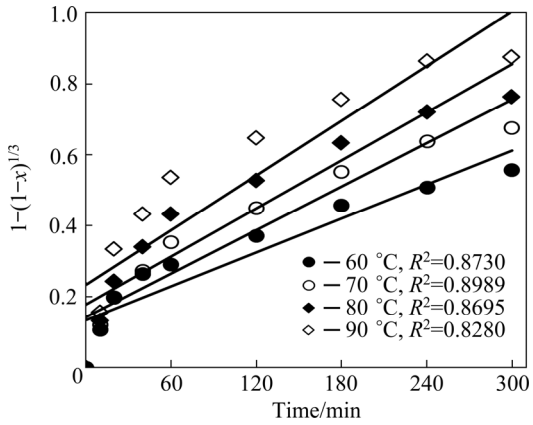

Fig. 11 Plot of $1-(1-x)^{1/3}$ against time at different temperatures

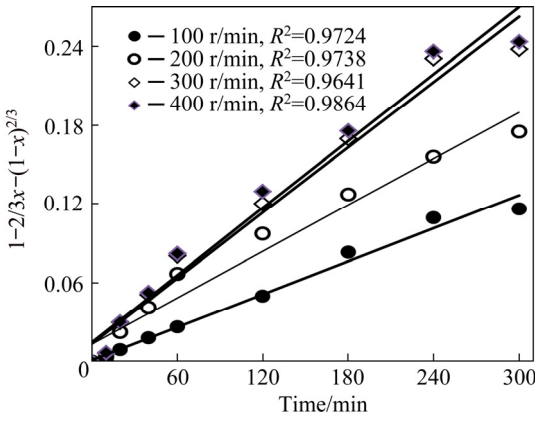

Fig. 13 Plots of $1-2/3x-(1-x)^{2/3}$ against time at different stirring speeds

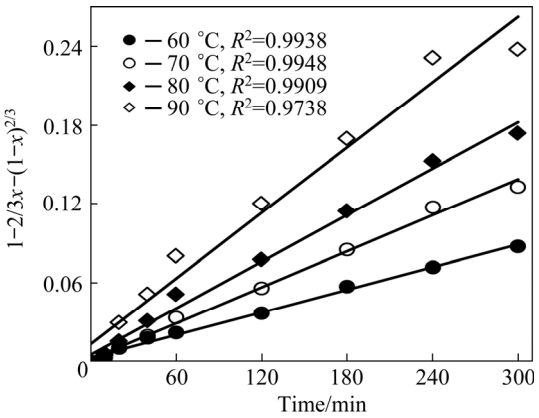

Fig. 12 Plot of $1-2/3x-(1-x)^{2/3}$ against time at different temperatures

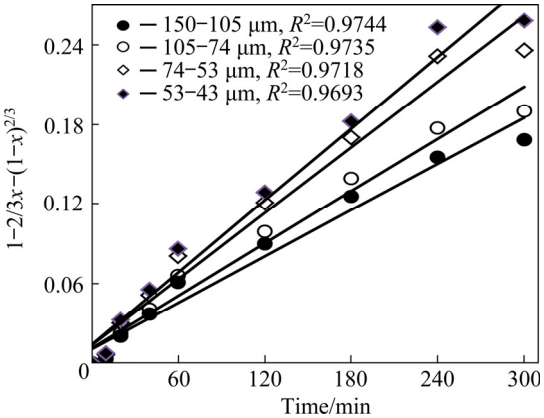

Fig. 14 Plots of $1-2/3x-(1-x)^{2/3}$ against time with different particle sizes

Similar to the activation energy plot, the order of the acid concentration was calculated based on the leached fractions of indium. As shown in Fig. 17, the reaction order for indium leaching from sulfuric acid is 2.41.

3.2 Fraction precipitation of copper and indium

3.2.1 Copper precipitation from reductive leachate

The reductive leaching experiments were carried out under the optimum conditions of stirring speed of 300 r/min, particle size of 74−105 μm, temperature of 90 °C and sulfuric acid concentration of 1.4 mol/L. The main components contained in the reductive leachate are illustrated in Table 4. The concentrations of Cu^{2+}, In^{3+}, Fe, Fe^{2+} and H_2SO_4 were 1.51, 0.097, 25.02, 23.67 and 36.73 g/L, respectively. The total iron concentration was significantly larger than that published in previous studies.

The precipitation of copper by iron from

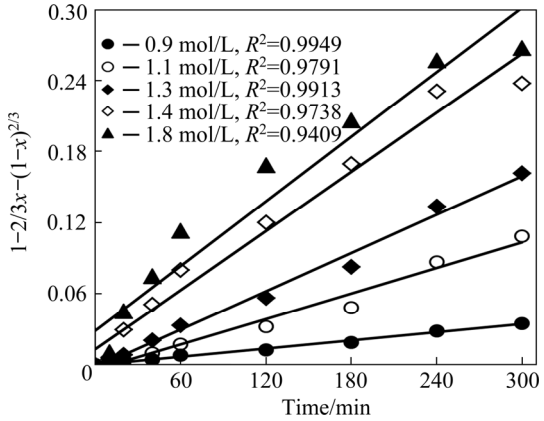

Fig. 15 Plots of $1-2/3x-(1-x)^{2/3}$ against time at different sulfuric acid concentrations

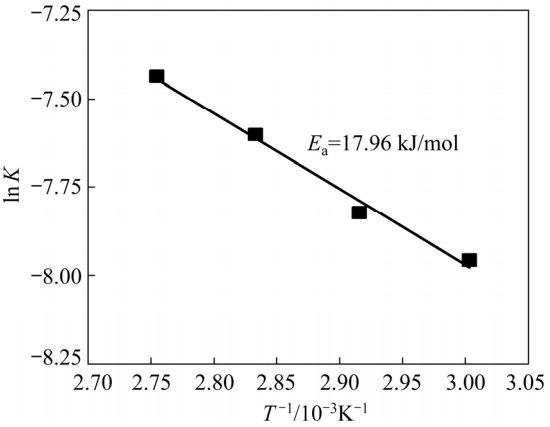

Fig. 16 Arrhenius plot for indium dissolution (K−Reaction rate constant)

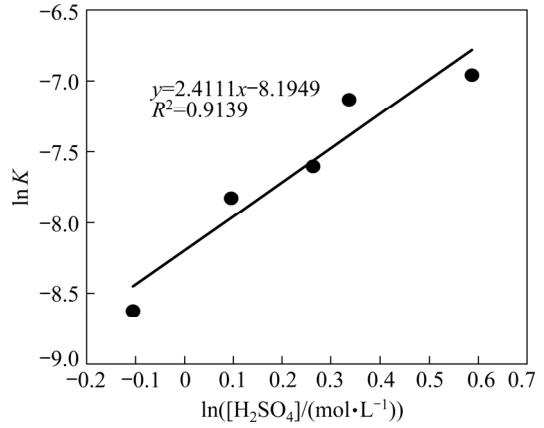

Fig. 17 Determination of reaction order with respect to sulfuric acid concentration (K−Reaction rate constant)

reductive leachate can be described as

$$Fe+Cu^{2+}=Fe^{2+}+Cu\downarrow \quad (6)$$

$$Fe+2Fe^{3+}=3Fe^{2+} \quad (7)$$

$$9Fe+6Cu^{2+}+2As^{3+}=9Fe^{2+}+2Cu_3As\downarrow \quad (8)$$

The stoichiometrically required amount of iron powder for copper precipitation was calculated according to Reactions (6) and (7). Copper precipitation experiments were carried out under optimum conditions obtained in a previous study at temperature of 70 °C, retention time of 25 min, and 1.2 times stoichiometrically-required amount of iron powder [29]. The concentrations of the main components in the copper precipitation supernatant are given in Table 4, and the precipitation efficiencies of copper and arsenic from the solution were 99.8% and 99.2%, respectively. A significant amount of arsenic can be removed by this step, and its concentration in the copper precipitation supernatant was only 2 mg/L, avoiding the formation of dangerous H_3As in the next indium cementation step by zinc powder. It was observed that there were no detectable zinc and indium losses at this step.

Table 4 Concentrations of main components in solution (g/L)

Component	Reductive leachate	Copper precipitation supernatant	pH adjusted supernatant
Zn^{2+}	103.2	103.5	131.9
Cu^{2+}	1.51	0.003	0.056
In^{3+}	0.097	0.097	0.104
Fe	25.02	27	27.22
Fe^{2+}	23.67	25.72	25.85
H_2SO_4	36.73	36.55	−
As^{3+}	0.22	0.002	0.013

3.2.2 Indium recovery from solution

The pH of copper precipitation supernatant was first adjusted to 4.0 with zinc calcine, and then, to optimize the quantity of zinc powder needed, precipitation experiments were carried out at temperature of 80 °C and reaction time of 60 min under different initial zinc powder concentrations of 3, 4, 5, 6 and 7 g/L. The experimental results present in Table 5 show that an increase in the initial zinc powder concentration from 3 to 6 g/L produced an obvious increase in the indium precipitation efficiency from 70.52% to 98.90%. Further increase of the initial zinc powder concentration to 7 g/L had little effect on the indium precipitation efficiency, and excessive addition of zinc powder reduced the indium content in the precipitate.

Table 5 Experiment results for indium precipitation from solution

Initial zinc powder concentration/ ($g \cdot L^{-1}$)	Unprecipitated indium concentration in solution/ ($mg \cdot L^{-1}$)	Indium precipitation efficiency/ %	Content of indium in precipitate/ %
3	32	70.52	1.74
4	19	82.39	1.96
5	5	95.07	2.3
6	1	98.9	2.41
7	<1	98.97	2.15

Thus, over 98% of indium can be selectively separated from ferrous and zinc sulphate leaching solutions, and the indium-rich precipitate, which has an indium content of approximately 2.4%, can be further treated by the acid leaching−solvent extraction−electrowinning process to produce pure indium.

4 Conclusions

(1) The zinc leaching residue and zinc sulfide concentrate used in the present study have a higher iron content than conventional zinc ore. The main mineralogical phases are sphalerite (ZnS) and marmatite ($Zn_2Fe_3S_5$) in zinc sulfide concentrate and zinc ferrite ($ZnFe_2O_4$) in HIZLR.

(2) A stirring speed of 300 r/min was sufficient to eliminate the effects of stirring speed on the kinetics. The particle size within the size range studied had a slight effect on indium dissolution. Temperature and the sulfuric acid concentration had pronounced influences on indium dissolution. As the temperature and sulfuric acid concentration increased, the indium leaching rate was greatly improved. More than 95% of indium was extracted under the optimum conditions.

(3) The shrinking core model was used to describe the dissolution kinetics of indium in sulfuric acid solutions well. The results showed that the indium leaching process was controlled by the diffusion through the solid product layer, with the activation energy of 17.96 kJ/mol. The order of the reaction with respect to the sulfuric acid concentration was determined as 2.41.

(4) Valuable metals of copper and indium were selectively separated from the leaching solution by fraction precipitation. Over 99% of copper and 98% of indium were precipitated from the solution by iron and zinc powder, respectively. The reductive leaching−fraction precipitation process is an effective method by which indium can be efficiently extracted from HIZLR and enriched in the precipitate.

Acknowledgments

The authors are grateful for the financial supports from the National Key Research and Development Plan of China (No. 2021YFC2902801), and the National Natural Science Foundation of China (Nos. 52064034, 51664038).

References

[1] ZHANG Kai-hua, WU Yu-feng, WANG Wei, LI Bin, ZHANG Yi-nan, ZUO Tie-yong. Recycling indium from waste LCDs: A review [J]. Resources Conservation and Recycling, 2015, 104: 276−290.

[2] THIQUYNHXUAN L, XIAO Bi-quan, JU Shao-hua, PENG Jin-hui, JIANG Feng. Separation of indium from impurities in T-type microreactor with D2EHPA [J]. Hydrometallurgy, 2019, 183: 79−86.

[3] ALFANTAZI A M, MOSKALYK R R. Processing of indium: A review [J]. Minerals Engineering, 2003, 16: 687−694.

[4] COOK N J, CIOBANU C L, WILLUAMS T. The mineralogy and mineral chemistry of indium in sulphide deposits and implications for mineral processing [J]. Hydrometallurgy, 2011, 108: 226−228.

[5] HOLLOWAY P C, ETSELL T H, MURLAND A L. Roasting of La Oroya zinc ferrite with Na_2CO_3 [J]. Metallurgical and Materials Transactions B−Process Metallurgy and Materials Processing Science, 2007, 38(5): 781−791.

[6] LI Xing-bin, WEI Chang, DENG Zhi-gan, LI Cun-xiong, FAN Gang, RONG Hao, ZHANG Fan. Extraction and separation of indium and copper from zinc residue leach liquor by solvent extraction [J]. Separation and Purification Technology, 2015, 156: 348−355

[7] YAN Huan, CHAI Li-yuan, PENG Bing, LI Mi, PENG Ning, HOU Dong-ke. A novel method to recover zinc and iron from zinc leaching residue [J]. Minerals Engineering, 2014, 55: 103−110.

[8] ÖZVERD A, ERDEM M. Environmental risk assessment and stabilization/solidification of zinc extraction residue. I: Environmental risk assessment [J]. Hydrometallurgy, 2010, 100: 103−109.

[9] MIN Xiao-bo, XIE Xian-de, CHAI Li-yuan, LIANG Yan-jie, LI Mi, KE Yong. Environmental availability and ecological risk assessment of heavy metals in zinc leaching residue [J]. Transactions of Nonferrous metals society of China, 2013, 23(1): 208−218.

[10] ALEX T C, KALINKIN A M, NATH S K, GUREVICH B I, KALINKINA E V, TYUKAVKINA V V, KUMAR S. Utilization of zinc slag through geopolymerization: Influence of milling atmosphere [J]. International Journal of Mineral Processing, 2013, 123: 102−107.

[11] SETHURAJAN M, HUGUENOT D, JAIN R, LENS P N L,

HORN H A, FIGUEIREDO L H A, HULLEBUSCH E D V. Leaching and selective zinc recovery from acidic leachates of zinc metallurgical leach residues [J]. Journal of Hazardous Materials, 2017, 324: 71−82.
[12] AKCIL A, CIFTCI H. Metals recovery from multimetal sulphide concentrates ($CuFeS_2$−PbS−ZnS): Combination of thermal process and pressure leaching [J]. International Journal of Mineral Processing, 2003, 71: 233−246.
[13] LI Cun-xiong, WEI Chang, XU Hong-sheng, LI Min-ting, LI Xing-bin, DENG Zhi-gan, FAN Gang. Oxidative pressure leaching of sphalerite concentrate with high indium and iron content in sulfuric acid medium [J]. Hydrometallurgy, 2010, 102: 91−94.
[14] DUTRIZAC J E. The dissolution of sphalerite in ferric sulfate media [J]. Metallurgical and Materials Transactions B−Process Metallurgy and Materials Processing science, 2006, 37(2): 161−171.
[15] SANTOS S M C, MACHADO R M, CORREIA M J N, REIS T A, ISMAEL M R C, CARVALHO J M R. Ferric sulphate/chloride leaching of zinc and minor elements from a sphalerite concentrate [J]. Minerals Engineering, 2010, 23: 606−615.
[16] ZHANG Yan-juan, LI Xuan-hai, PAN Liu-ping, WEI Yan-song, Liang Xin-yuan. Effect of mechanical activation on the kinetics of extracting indium from indium-bearing zinc ferrite [J]. Hydrometallurgy, 2010, 102: 95−100.
[17] MARTIN M, JANNECK E, KERMER R, PATZIG A, REICHEL S. Recovery of indium from sphalerite ore and flotation tailings by bioleaching and subsequent precipitation processes [J]. Minerals Engineering, 2015, 75: 94−99.
[18] JOWKAR M J, BAHALOO H N, MOUSAVI S M, POURHOSSEIN F. Bioleaching of indium from discarded liquid crystal displays [J]. Journal of Cleaner Production, 2018, 180: 417−429.
[19] DHAWAN N, SAFARZADEH M S, BIRINCI M. Kinetics of hydrochloric acid leaching of smithsonite [J]. Russian Journal of Non-ferrous Metals, 2011, 52(3): 209−216.
[20] LI Shi-qing, TANG Mo-tang, HE Jing, YANG Sheng-hai, TANG Chao-bo, CHEN Yong-ming. Extraction of indium from indium-zinc concentrates [J]. Transactions of Nonferrous Metals Society of China, 2006, 16(6): 1448−1454.
[21] LI Cun-xiong, WEI Chang, XU Hong-sheng, DENG Zhi-gan, LIAO Ji-qiang, LI Xing-bin, LI Min-ting. Kinetics of indium dissolution from sphalerite concentrate in pressure acid leaching [J]. Hydrometallurgy, 2010, 105: 172−175.
[22] ZHANG Yan-juan, LI Xuan-hai, PAN Liu-ping, LIANG Xin-yuan, Li Xue-ping. Studies on the kinetics of zinc and indium extraction from indium-bearing zinc ferrite [J]. Hydrometallurgy, 2010, 100: 172−176.
[23] LUO Wen-bo, WANG Ji-kun, WANG Guo-wei. Pressure leaching kinetics of indium in zinc oxide dust [J]. Hydrometallurgy of China, 2016, 2: 106−109. (in Chinese)
[24] LI Xue-peng, LIU Da-chun, WANG Juan. Experimental and kinetic study on oxygen pressure acid leaching of indium from low-content indium-containing leaching residue [J]. Journal of Central South University (Science and Technology), 2018, 49(8): 1869−1877. (in Chinese)
[25] XIE Ke-qiang, YANG Xian-wan, WANG Ji-kun, YAN Jiang-feng, SHEN Qing-feng. Kinetic study on pressure leaching of high iron sphalerite concentrate [J]. Transactions of Nonferrous Metals Society of China, 2007, 17(1): 187−194.
[26] HAN Hai-sheng, SUN Wei, HU Yue-hua, TANG Hong-hu. The application of zinc calcine as a neutralizing agent for the goethite process in zinc hydrometallurgy [J]. Hydrometallurgy, 2014, 148: 120−126.
[27] SOUZA A D, PINA P S, LEAO V A, SILVA C A, SIQUEIRA P F. The leaching kinetics of a zinc sulphide concentrate in acid ferric sulphate [J]. Hydrometallurgy, 2007, 89: 72−81.
[28] KARIMI S, RASHCHI F, MOGHADDAM J. Parameters optimization and kinetics of direct atmospheric leaching of Angouran sphalerite [J]. International Journal of Mineral Processing, 2017, 162: 58−68.
[29] ZHENG Yu, DENG Zhi-gan, FAN Gang, WEI Chang, LI Xing-bin, LI Cun-xiong, LI Min-ting. Study on the reaction behavior of precipitation of Cu(II) and As(III) by metallic iron [J]. The Chinese Journal of Nonferrous Metals, 2019, 29(6): 1298−1307. (in Chinese)

铟的还原浸出动力学及分步沉淀选择性分离

李存兄，张兆闫，张耀阳，邓志敢，吉文斌，林晓坦

昆明理工大学 冶金与能源工程学院，昆明 650093

摘　要：开展硫化锌精矿还原浸出高铁锌浸出渣高效浸铟及浸出液中铟选择性分离的研究。结果表明：在固体物料粒度 74~105 μm、反应温度 90 ℃、浸出时间 300 min、硫酸浓度 1.4 mol/L 的条件下，铟的浸出率达 95%以上。采用收缩核模型对还原浸出动力学进行分析，不同条件下的浸出实验结果表明反应受穿过固体产物层的扩散控制，活化能为 17.96 kJ/mol，相对于硫酸浓度的反应级数为 2.41。铁粉置换沉铜过程铜和砷的沉淀率均达 99%以上。98%以上的铟从含高亚铁离子浓度的硫酸锌溶液中选择性分离，获得铟含量约为 2.4%的富铟渣，经酸浸−萃取−电积工艺流程进一步处理后可得到纯铟。

关键词：还原浸出；高铁锌浸出渣；硫化锌精矿；动力学；铟沉淀

(Edited by Bing YANG)